



HAL
open science

In vitro evaluation of *Pseudomonas aeruginosa* chronic lung infection models: Are agar and calcium-alginate beads interchangeable?

Bruna Gaelzer Silva Torres, Rana Awad, Sandrine Marchand, William Couet, Frédéric Tewes

► To cite this version:

Bruna Gaelzer Silva Torres, Rana Awad, Sandrine Marchand, William Couet, Frédéric Tewes. In vitro evaluation of *Pseudomonas aeruginosa* chronic lung infection models: Are agar and calcium-alginate beads interchangeable?. *European Journal of Pharmaceutics and Biopharmaceutics*, 2019, 143, pp.35-43. 10.1016/j.ejpb.2019.08.006 . hal-02477575

HAL Id: hal-02477575

<https://hal.science/hal-02477575>

Submitted on 20 Jul 2022

HAL is a multi-disciplinary open access archive for the deposit and dissemination of scientific research documents, whether they are published or not. The documents may come from teaching and research institutions in France or abroad, or from public or private research centers.

L'archive ouverte pluridisciplinaire **HAL**, est destinée au dépôt et à la diffusion de documents scientifiques de niveau recherche, publiés ou non, émanant des établissements d'enseignement et de recherche français ou étrangers, des laboratoires publics ou privés.



Distributed under a Creative Commons Attribution - NonCommercial 4.0 International License

1 *In vitro* evaluation of *Pseudomonas aeruginosa* chronic lung
2 infection models: Are agar and calcium-alginate beads
3 interchangeable?
4
5
6
7

8 Torres, Bruna Gaelzer Silva¹; Awad, Rana¹; Marchand, Sandrine^{1,2}; Couet, William^{1,2}; Tewes,
9 Frederic¹.

10

11

12 ¹ - Inserm U1070, Université de Poitiers, CHU de Poitiers, 1 rue Georges Bonnet, 86073 POITIERS

13 Cedex 9, France.

14 ² - Laboratoire de Toxicologie-Pharmacocinétique, CHU of Poitiers, 2 rue de la Milétrie, 86000

15 Poitiers, France

16

17 Corresponding authors at: INSERM, U1070, UFR de Médecine Pharmacie, Université de Poitiers, 1

18 rue Georges Bonnet, TSA 51106, 86073 Poitiers Cedex 9, France

19 E-mail address: ftewes@univ-poitiers.fr

20 Abstract

21 Animal models of chronic lung infection with *P. aeruginosa* (*PA*) are useful tools to improve antibiotic
22 (ATB) treatment. Two main models based on the pulmonary instillation of *PA* embedded in agar or
23 calcium-alginate beads are currently used. However, these two polymers used to prepare the beads
24 have different properties; for example, agar is a neutral polysaccharide while alginate is anionic. We
25 hypothesized that the effect of an ATB on *PA* entrapped in agar or calcium-alginate beads depends on
26 its physicochemical properties, including charge, and concentration. To test this hypothesis, *PA*s were
27 entrapped in agar or calcium-alginate beads dispersed in a growth medium containing either
28 tobramycin (TOB), selected as a cationic ATB, or ciprofloxacin (CIP) selected as a neutral zwitterionic
29 ATB. *In vitro*, time-kill curves evaluating the efficacy of ATBs over time were performed by measuring
30 the light emitted by a bioluminescent *PA* for 42 hours in the presence of ATB concentrations ranging
31 from 0 to 100 times the MIC. In the presence of CIP, time-kill curves obtained with *PA* trapped in agar
32 or calcium-alginate beads were comparable, whatever the CIP concentration used. In the presence of
33 TOB, a clear difference was observed between the kill curves obtained with *PA* embedded in agar or
34 calcium-alginate beads. While *PA* trapped within agar displayed the same susceptibility than the
35 planktonic one, it was unresponsive to TOB for concentrations up to 1-fold MIC when trapped in
36 calcium-alginate. At 10-fold the TOB's MIC, the luminescence emitted by *PA01* in the agar beads was
37 reduced by 95% after 40 h, whereas it returned to the same initial value for *PA01* trapped in alginate-
38 based beads. The reduction in TOB efficiency was even greater when alginate-based beads were
39 dispersed in a mucus-simulating medium. These results show that the agar and alginate beads models
40 can be interchangeable only for uncharged ATB, such as CIP, but not for cationic ATB, like TOB. *In vitro*
41 experiments performed in this study could be a quick way to evaluate the effect of each model on a
42 given ATB before performing animal experiments.

43 **1. Introduction**

44 Animal models of chronic lung infection with *Pseudomonas aeruginosa* (*PA*) are useful tools to
45 improve antibiotic (ATB) treatment of these infections in human. The first murine model of chronic
46 bronchopulmonary infection with *PA* was developed by pulmonary instillation of *PA* embedded in agar
47 beads [1]. The aim of embedding *PA* within agar beads is to physically restrain the bacteria in the
48 airways by creating an interface between the bacteria and the host that protects them from each
49 other. This leads to persistent stimulation of host defenses and to inflammation that mimics the
50 pathophysiology of chronic lung infection observed in human [2]. A second model was then developed
51 using calcium-alginate beads to replace the agar beads. These alginate-based beads better simulate
52 *in vivo* conditions in which mucoid *PA* are embedded within self-produced alginate found in pulmonary
53 biofilms in cystic fibrosis (CF) patients [3-5].

54 Both models are still used today to evaluate the efficacy of ATB to treat chronic lung infections [2, 4,
55 6-8]. However, these two polymers used to form the beads have different properties; for example,
56 agar is a neutral polysaccharide while alginate is anionic. Thus, they could interact differently with
57 ATBs, especially in relation with their charge, and thereby might alter their diffusion, binding, and as
58 a result their efficacy. Therefore, using TOB and CIP as representatives of cationic and non-ionized
59 ATBs, respectively, the aim of this study was to determine whether these models have an impact on
60 the efficiency of some ATBs or whether they can be considered interchangeable. Indeed, we
61 hypothesized that the effect of an ATB on bacteria entrapped in agar or calcium-alginate beads could
62 depend on its physicochemical properties, such as ATB charge and concentration. To test this
63 hypothesis, *in vitro* time-kill curves-like, measuring ATB efficacy over the time have been performed
64 by recording the light emitted by a bioluminescent *PA* for 42 hours for different TOB and CIP
65 concentrations.

66 2. Methods

67 2.1. Materials

68 A *P. aeruginosa* PAO1 strain, hereafter referred as PAO1, which was made bioluminescent by
69 chromosomal integration of the luxCDABE operon, was kindly provided by Professor Patrick Plesiat
70 (Centre National de Référence de la résistance aux antibiotiques, Centre Hospitalier Universitaire de
71 Besançon, France). Tobramycin (TOB) and ciprofloxacin (CIP), were purchased from Sigma Aldrich
72 (France).

73 2.2. Luminescence kinetics using planktonic *P. aeruginosa*

74 PAO1 was grown overnight in cation-adjusted Mueller-Hinton Broth (MHB; Sigma-Aldrich, France) in
75 an orbital shaker at 37°C. The optical density of a suspension measured at 600 nm (OD₆₀₀) was adjusted
76 to 0.03 ($\approx 1-2 \times 10^7$ cells/mL)[9] in MHB (after subtracting MHB absorbance value) and the suspension
77 was incubated at 37°C. **Once the exponential phase of growth was reached (approximately 3 hours,**
78 **evaluated by measuring the OD₆₀₀ every 15 min), 100 μ L of the bacterial suspension, having a**
79 **concentration adjusted to obtain an initial luminescence of 10 000 RLU, were dispersed in the wells of**
80 **a low-binding (to avoid biofilm formation), white, flat-bottom, 96-well microplate (Greiner®, ref:**
81 **655904, France).** Then, 100 μ L of MHB containing the 2 times concentrated ATB was added. ATBs
82 concentrations used, expressed in number of times the minimum inhibitory concentration (MIC; 0.025
83 mg/L for CIP and 0.5 mg/L for TOB) were 100, 50, 25, 10, 5, 2, 1, 0.5, 0.25, and 0. The plates were
84 sealed with a clear, gas permeable, moisture barrier membrane (4titude®, ref: 4ti-0516/96) and
85 luminescence was recorded every 30 minutes for 42 hours at 37°C using an Infinite M200 Pro
86 microplate reader (Tecan, France). **The use of luminescence enables each well to be used as its own**
87 **control over time, thus limiting the number of wells required in the study and minimizing well-to-well**
88 **variations by normalization. Thus, luminescence values recorded at different times were normalized**
89 **by the initial luminescence recorded for each well so that all kinetics curves start at 1 on the y-axis.**
90 Plates were shaken before each measurement (n= 12-16).

91 2.3. Luminescence kinetics using biofilms adsorbed on an abiotic surface

92 For biofilms formation, the OD₆₀₀ of an overnight suspension was adjusted to 0.03 in MHB and 200 μL
93 were dispensed in the wells of **high-binding** (to facilitate bacteria adherence), white, flat-bottom 96-
94 well microplate (Greiner®, ref: 655074, France). Plates were sealed using an air-permeable membrane
95 and incubated in an orbital shaker at 37°C. After 24 h, the supernatants were removed, and the wells
96 were rinsed 4 times with 150 μL of PBS pH 7.4. The washing procedure is critical, with the main
97 emphasis on preserving biofilm integrity. Then, 200 μL of MHB containing the 1 time concentrated
98 ATB were added. The plates were sealed with a clear, gas permeable, moisture barrier membrane,
99 and then the luminescence was recorded every 30 minutes for 42 hours at 37°C using the microplate
100 reader (Tecan, France) (n= 12-16). **In the presence of planktonic bacteria, the value of the initial**
101 **luminescence was set around 10 000 RLU in each well by adjusting the bacteria concentration. For**
102 **biofilms, the initial number of bacteria could not be changed and the initial luminescence values used**
103 **to normalize the data ranged from 2000 to 5000 RLU.**

104 2.4. Luminescence kinetics using *P. aeruginosa* entrapped in polysaccharides beads

105 2.4.1. Agar beads preparation

106 Agar beads loaded with *PAO1* were prepared using an adapted version of the method described by
107 Growcott *et al.* [2]. Fresh *PAO1* suspension prepared in MHB was cultured to exponential growth
108 phase and then adjusted to an OD₆₀₀ of 0.3. Two mL of this suspension was washed with PBS pH 7.4
109 and bacteria were concentrated in 1 mL of PBS. Then, this suspension was dispersed in 9 mL of 2%
110 m/v molten agar solution (agar; VWR, France), which was then emulsified into 100 mL of warmed
111 (48°C) paraffin oil (Sigma Aldrich, France) containing 0.01% v/v of sorbitan monooleate (SPAN®60,
112 Sigma Aldrich, France) using a mechanical stirrers model RZR-2021 (Heidolph, France) at 1300 rpm.
113 Then, under moderate mixing (300 rpm), the emulsion was cooled for 1 hour by pouring pieces of ice
114 around the beaker to produce agar beads, which were centrifuged at 5,000 g for 10 min, and then
115 washed 4 times with PBS pH 7.4. Sterile beads were prepared under the same conditions by using 1
116 mL of PBS instead of 1mL of bacterial suspension and their size distribution was determined by laser

117 light diffraction (Microtrac® X100 particle size analyzer). Evaluations of the size of some *PAO1*-loaded
118 beads were performed by microscopic observation.

119 2.4.2. Alginate beads preparation

120 Alginate (Alginic acid sodium salt from brown algae; Sigma Aldrich, France) beads were produced using
121 the same emulsification process than for agar beads preparation. However, after the emulsification
122 step, the gelation of the droplets containing the alginate at a concentration of 2% m/v was induced by
123 adding dropwise and under stirring 20 mL of 0.1M TRIS-HCl buffer pH 7 containing 0.1M of CaCl₂ to
124 the emulsion. After 2 hours of moderate stirring (300 rpm), beads were centrifuged at 5,000 g for 10
125 min and then washed 4 times with a 0.9 % m/v NaCl solution. Sterile beads were prepared by the same
126 method to determine their size distribution.

127 2.4.3. Time-luminescence kinetics with polymer beads

128 *PAO1* loaded into freshly prepared beads were dispersed in MHB and bioluminescence was adjusted
129 to obtain the same luminescence intensity than with the experiments done using planktonic bacteria
130 (\approx 10000 RLU). Then 100 μ L of beads suspension was dispensed in a low-binding (to avoid biofilm
131 formation), white, flat-bottom, 96-well microplates (Greiner®, ref: 655904, France), followed by 100
132 μ L of 2 times concentrated ATB solution in MHB. The plates were sealed with a clear, gas permeable,
133 moisture barrier membrane and luminescence was recorded every 30 minutes for 42 hours at 37°C
134 using the microplate reader (Tecan, France) (n= 12-16).

135 In traditional *in-vivo* models of *PA* chronic lung infection, polymer beads are instilled into the animal
136 lungs, and after 3-4 days when the bacterial burden is stable, they are exposed to ATB [4]. Under these
137 conditions, biofilms can be created inside the beads before being in contact with ATB [10]. Thus, to
138 evaluate the effect of biofilm formation within the beads, *PAO1*-loaded agar beads were incubated
139 under stirring for 48 hours at 37°C in MHB, and then washed 4 times with PBS pH 7.4. Afterward, the
140 luminescence of the bead suspension was adjusted to 10000 RLU in MHB and luminescence kinetics
141 were recorded in the presence of various TOB concentrations as described above.

142 Most of the *PA* chronic lung infections are associated with the presence of abundant mucus which can
143 be an additional barrier to ATB efficacy [11, 12]. To test the effect of the components of the mucus on
144 the calcium-alginate beads model, additional luminescence kinetics were performed by dispersing the
145 beads in an artificial sputum medium (ASM) instead of the MHB, in the presence of different TOB
146 concentrations. ASM was prepared following the protocol of Sriramulu *et al.* [13]. It contains 5 g/L of
147 mucin from porcine stomach (Sigma-Aldrich, France), 4 g/L of low molecular-weight salmon sperm
148 DNA (Sigma-Aldrich), 5.9 mg/L of the iron-chelator diethylene triamine pentaacetic acid (Sigma-
149 Aldrich), 5 g/L of NaCl (Sigma-Aldrich), 2.2 g/L of KCl (Sigma-Aldrich), 5% (v/v) of egg yolk emulsion
150 (Sigma-Aldrich) and 5 g/L of casein amino acids (Sigma-Aldrich).

151 2.5. Antibiotic diffusion measurements

152 Effective diffusivities of CIP and TOB within the two gels were determined by assaying the amount of
153 ATB that crossed a layer of gel as a function of time. In these experiments, 2% m/v agar or calcium-
154 alginate gel layers were prepared in membrane-free Thincerts® 24-well plate inserts (Greiner bio-one;
155 France). The thickness of the gel layers was adjusted to 0.45 cm by trimming off the excess of gel.
156 Inserts were placed in a 24-well plate and equilibrated for 1 hour at 37°C with 1.2 mL and 0.25 mL of
157 TRIS-HCl buffer pH 7 in the acceptor and donor compartment, respectively. Then, TRIS-HCl buffer in
158 the acceptor compartment was removed and replaced by a TRIS solution containing the ATB at a
159 concentration of 10 or 100 times the MIC. At different times (10, 20, 30, 40, and 60 min for CIP and
160 30, 60, 90, 120, and 150 min for TOB) 500 µL of the acceptor compartment was removed and replaced
161 by the same volume of warm, ATB free, TRIS buffer pH 7 (n= 4 per ATB concentration). ATBs
162 concentrations were determined using the analytical methods described on 2.7. The cumulative
163 amount of ATB per centimeter square (ng/cm²) versus time was plotted to check linearity and calculate
164 the slope (ng/sec/cm²). Apparent permeability (cm/sec) was calculated by dividing the slope by the
165 donor compartment initial ATB concentration (ng/cm³). Effective diffusivity (cm²/sec) was calculated
166 by dividing the apparent permeability by the gel layer thickness (cm).

167 2.6. TOB binding to alginate

168 Calcium-alginate gels were formed by adding 200 μL of alginate solution at 2% m/v in Eppendorf tubes
169 and then, after centrifugation, 600 μL of 0.1M TRIS-HCl buffer pH 7 containing 0.1M of CaCl_2 . After 4
170 hours of gelation, 550 μL of liquid was removed and 500 μL of TOB solution in TRIS-HCl was added.
171 After incubation for 7 days at 37 $^\circ\text{C}$, the free TOB concentration in the liquid phase in equilibrium with
172 the gel was determined by the LC-MSMS method described below. A control without alginate gel was
173 treated in the same conditions to evaluate the TOB stability and plastic tube binding. No significant
174 change in TOB concentration was observed in the control over the 7 days. The data for three
175 experiments on binding of TOB to calcium-alginate gel were analyzed as described by Nichols et al.
176 [14] using a linear adsorption isotherm equation, $B = RC$, where B is the amount of TOB bound in a
177 unit volume (in $\mu\text{g}/\text{mL}$), C is the free TOB concentration ($\mu\text{g}/\text{mL}$), and R is a constant of proportionality.

178 2.7. Antibiotic assays

179 2.7.1. CIP assay

180 CIP was assayed using an Infinite M200 Pro microplate reader (Tecan, France) as a fluorimeter. Stock
181 solutions of CIP in acidic water with 0.1 mM HCl were prepared at 1 mg/mL. Standard solutions having
182 CIP concentrations of 100, 50, 25, 10, 5, and 1 ng/mL as well as QC solutions having CIP concentrations
183 of 75, 15, and 2.5 ng/mL were prepared in PBS pH 7.4 or TRIS-HCl pH 7. Then, 250 μL of these solutions
184 and samples were added in the wells of a low-binding, white, 96-well microplate (Greiner[®], ref:
185 655904, France) and the fluorescence intensity at 430 nm was measured after excitation at 278 nm.
186 Coefficients of determination of linear regressions of calibration curves were higher than 0.99 and QC
187 and standards biases were lower than 15%.

188 2.7.2. TOB assay

189 TOB was assayed using an LC-MSMS method previously described [15]. Briefly, a Waters Alliance 2695
190 separation module coupled with a Waters Micromass Quattro micro API tandem mass spectrometer
191 was used. Chromatographic separation was done with an X bridge C18 column (5.0 μm , 150 by 2.1
192 mm); Waters, St-Quentin en Yvelines, France) and a mobile phase composed of 0.1% (vol/vol) formic
193 acid in water and 0.1% formic acid in acetonitrile (75:25, vol/vol) flowing at 0.2 $\text{ml}\cdot\text{min}^{-1}$.

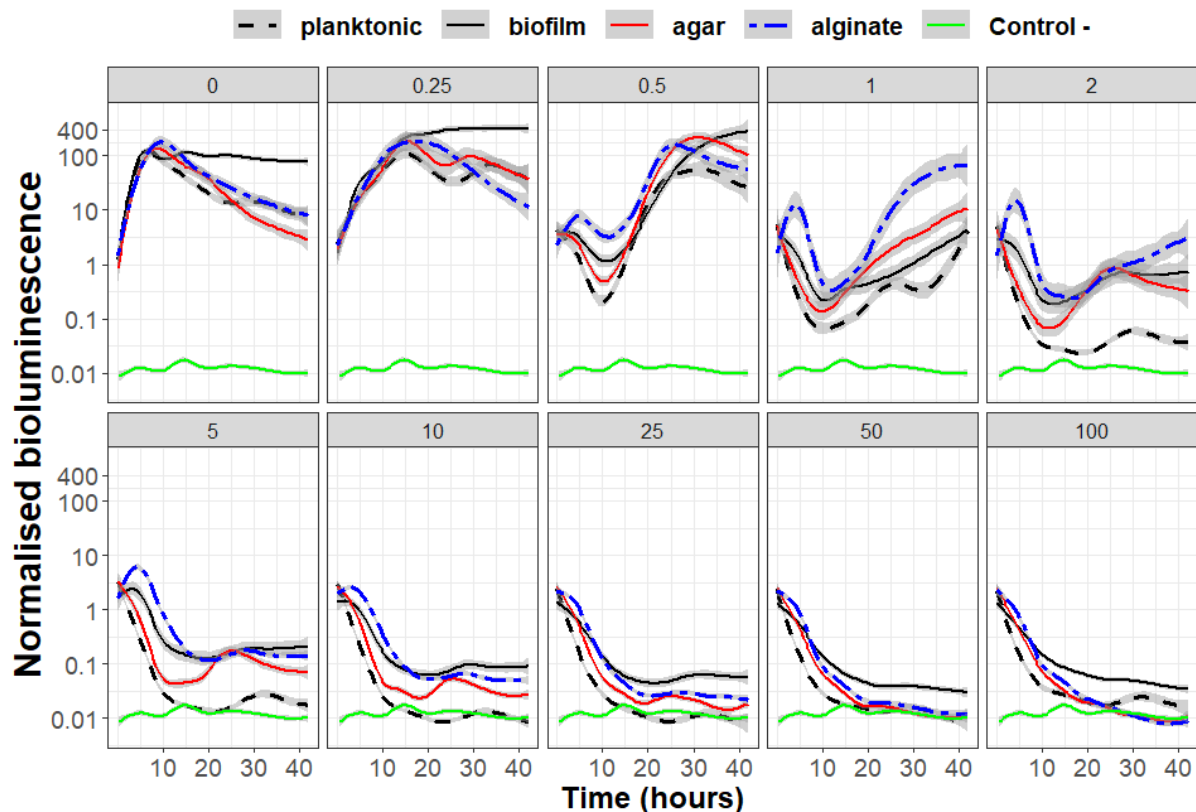
194 Quantification was performed in the positive-ion mode with multiple-reaction monitoring of m/z
195 transitions 468.2 → 163.1 for TOB and 448.2 → 160.2 for sisomycin, the internal standard (1 µg/mL).
196 TOB concentrations of the standard solutions were 1000, 750, 500, 100, 25, 5, 2.5, and 1 ng/mL and
197 750, 100, and 2.5 ng/mL for the QC solutions. Coefficients of determination of linear regressions of
198 calibration curves were higher than 0.99 and QC and standards biases were lower than 15%.

199 2.8. Data analysis

200 All data analyses were performed using the R software version. 3.4 and the package “ggplot2 v. 3.10”
201 was used to plot smoothed mean luminescence values versus time using a generalized additive model
202 (GAM) **as smoothing method**. The shaded area around the mean value curve is the 95% confidence
203 level interval for the mean values predicted from the GAM smoothing model.

204 **3. Results**

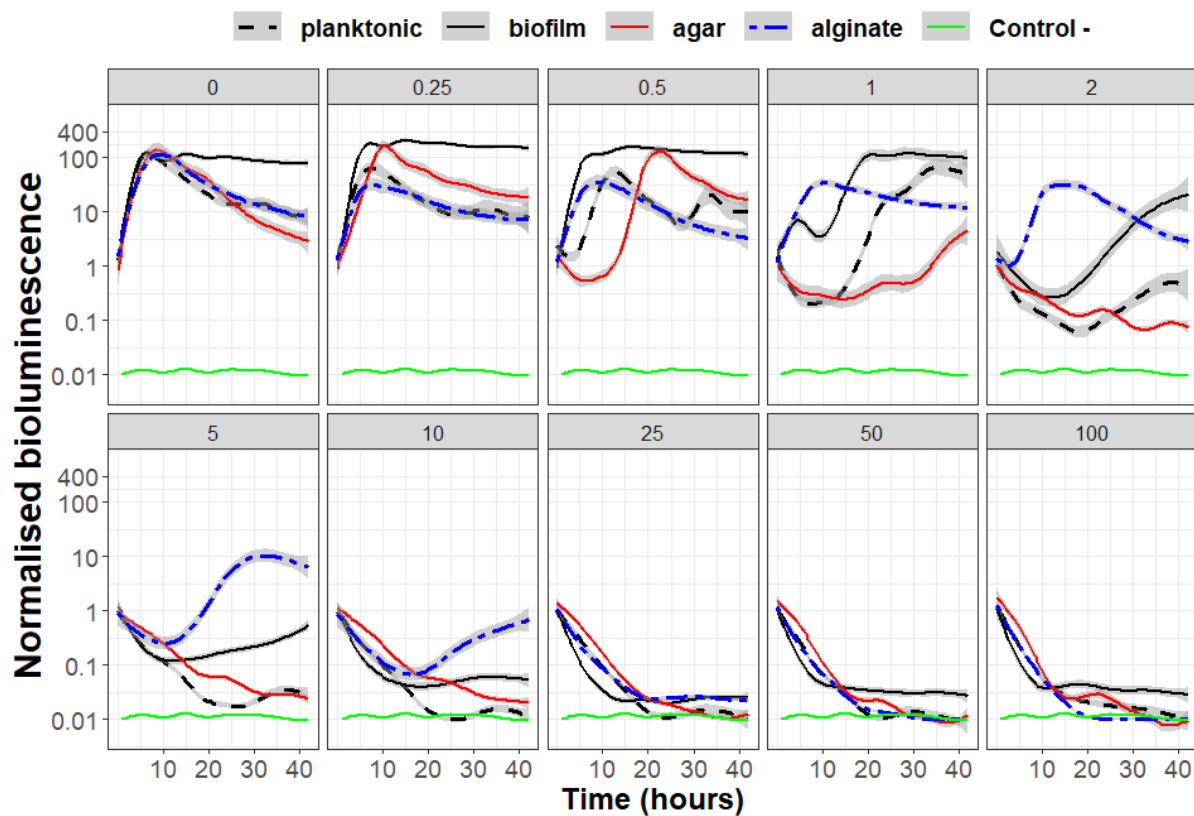
205 **Bioluminescence kinetics of planktonic PA and adsorbed biofilms of PA in the presence of CIP or**
206 **TOB.** In order to obtain references for comparing the data obtained with PAs trapped in polymer
207 beads, luminescence kinetics were first recorded for planktonic PAs and PAs adsorbed on plastic
208 surfaces as biofilms in the presence of CIP (Figure 1) or TOB (Figure 2).



209 **Figure 1: Time-luminescence curve obtained with planktonic PAO1 (black dashed lines), biofilms of**
210 **PAO1 (black solid lines), PAO1 trapped in agar beads (red solid lines), or PAO1 trapped in calcium-**
211 **alginate (blue two-dash lines) beads exposed to various CIP concentrations in MHB expressed in the**
212 **number of times the MIC (Top of each graph). The green horizontal curve (Control -) is the signal**
213 **obtained in the absence of bacteria. For each well, luminescence intensity was normalized to the**
214 **value measured at time zero. The gray band around the lines is the 95% confidence level interval of**
215 **the mean values predicted from the GAM smoothing model (n = 6-16). The mean values between**
216 **different conditions are significantly different in the absence of overlapping of these gray-shaded**
217 **areas.**

219 In the absence of ATB, luminescence produced by planktonic PAO1 or biofilms of PAO1 increased
220 similarly for 5 hours (Figure 1 and 2). For biofilms, the luminescence was then stable for the time of
221 the experiment, while it decreased slowly for the planktonic bacteria. The addition of CIP at a low

222 concentration, e.g. 0.25 times the MIC, decreased the bacteria growth rate in both growing mode and
 223 a plateau was reached only after 15 hours. At this CIP concentration, biofilms had higher normalized
 224 luminescence at the plateau compared to values got without ATB. For CIP concentrations comprised
 225 between 2 to 100 times the MIC, biofilms formed on the bottom of 96-well plates were less susceptible
 226 to CIP than the planktonic bacteria (Figure 1). A higher luminescence decrease rate and a greater
 227 extent of the luminescence decrease were obtained with the planktonic bacteria compare to biofilms.



228
 229 **Figure 2: Luminescence kinetics obtained with planktonic *PAO1* (black dashed lines), biofilms of**
 230 ***PAO1* (black solid lines), *PAO1* trapped in agar beads (red solid lines), or *PAO1* trapped in calcium-**
 231 **alginate (blue two-dash lines) beads exposed to various TOB concentrations in MHB expressed in**
 232 **the number of times the MIC (Top of each graph). The green horizontal curve (Control -) is the signal**
 233 **obtained in the absence of bacteria. For each well, luminescence intensity was normalized to the**
 234 **value measured at time zero. The gray band around the lines is the 95% confidence level interval of**
 235 **the mean values predicted from the GAM smoothing model (n = 6-16). The mean values between**
 236 **different conditions are significantly different in the absence of overlapping of these gray-shaded**
 237 **areas.**

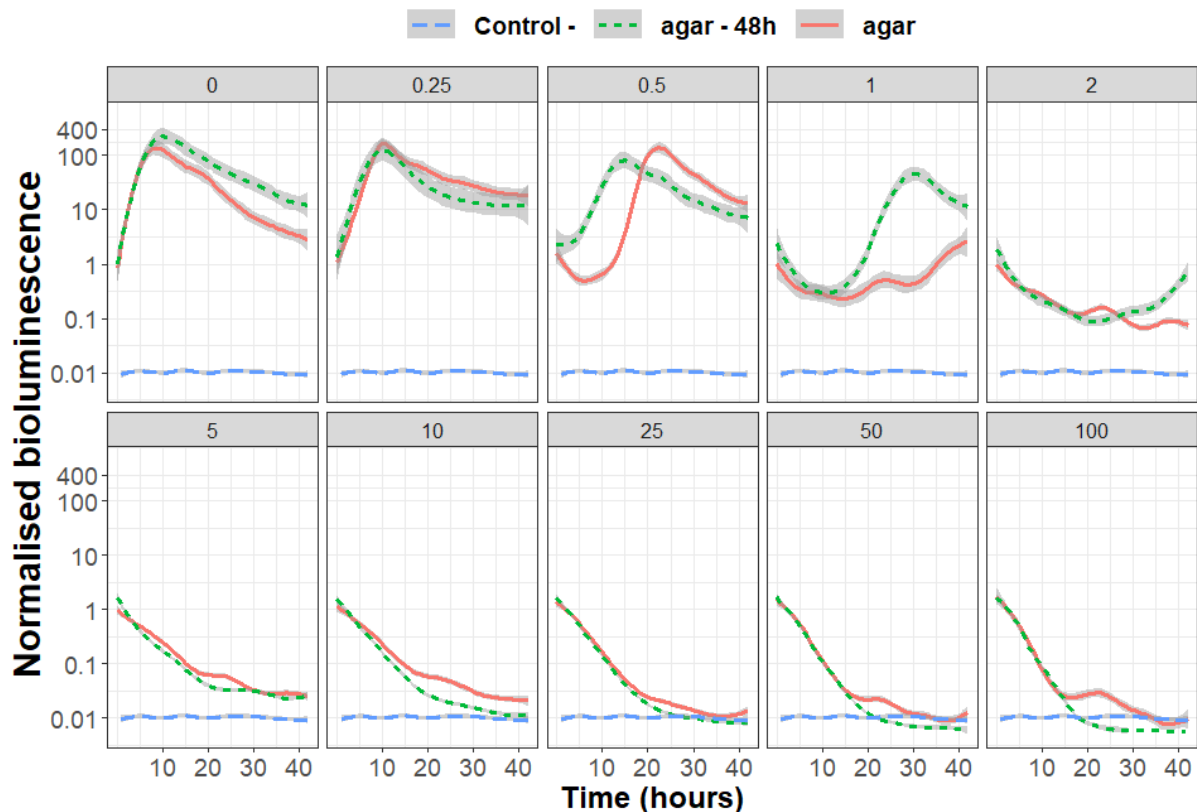
238 The overall time-luminescence profiles obtained with CIP or TOB against planktonic or biofilm of *PAO1*
239 were similar and planktonic bacteria were generally more susceptible to both ATBs than biofilms
240 (Figure 1 and 2). However, for ATB concentrations below 25 times the MIC, biofilms were less sensitive
241 to TOB than CIP. For example, no effects were observed with biofilms exposed to TOB at
242 concentrations up to 0.5 times the MIC (Figure 2), whereas CIP showed an effect from 0.25 times the
243 MIC (Figure 1). In addition, for biofilms exposed to ATB concentrations ranging from 1 to 5 times the
244 MIC, greater luminescence rebounds were observed with TOB than with CIP.

245 **Bioluminescence kinetics of *PA* entrapped in agar or calcium-alginate beads.** Both types of beads
246 were prepared using a similar emulsification method and comparable monodisperse size distributions
247 were obtained (supplementary material 1). Their mean diameters of $68 \pm 23 \mu\text{m}$ and $81 \pm 27 \mu\text{m}$, for
248 calcium-alginate and agar, respectively, were not significantly different ($p = 0.58$, two-tailed t-test).

249 Luminescence kinetics acquired with *PAO1* trapped in agar or calcium-alginate beads were nearly
250 similar for all tested CIP concentrations (Figure 1). The only difference observed was an initial increase
251 in luminescence over the five first hours with the alginate beads, while the luminescence decreased
252 immediately with the agar ones for CIP concentrations between 0.5 and 10 times the MIC. Thus, no
253 effect of the polymer forming the beads was observed in the presence of CIP. For CIP concentrations
254 between 0.5 and 10 times the MIC, the luminescence profiles obtained with *PAO1* entrapped in both
255 types of beads were close to those obtained with biofilms adsorbed on the bottom of the 96-well
256 plates. However, for higher CIP concentrations, the profiles were similar to those obtained with
257 planktonic bacteria.

258 Although no effect of the type of beads used was observed on the CIP effectiveness, for certain TOB
259 concentrations, the luminescence profiles were changed depending on the type of beads. For TOB
260 concentrations lower than 0.5 times the MIC, and higher than 25 times the MIC, no effect of the
261 polymer was observed and the same profiles were obtained with agar or calcium-alginate beads
262 (Figure 2 - Supplementary materials 4). For these TOB concentrations ranges, the kinetics were similar
263 to those obtained with planktonic bacteria. However, between these TOB concentrations, *PAs*

264 entrapped in alginate-based beads were less susceptible to TOB than those entrapped in agar beads.
 265 For this TOB concentration range, *PA*s embedded in the alginate beads were also less susceptible to
 266 TOB than the bacteria present in the biofilms adsorbed on the bottom of the 96-well plates and the
 267 planktonic bacteria.

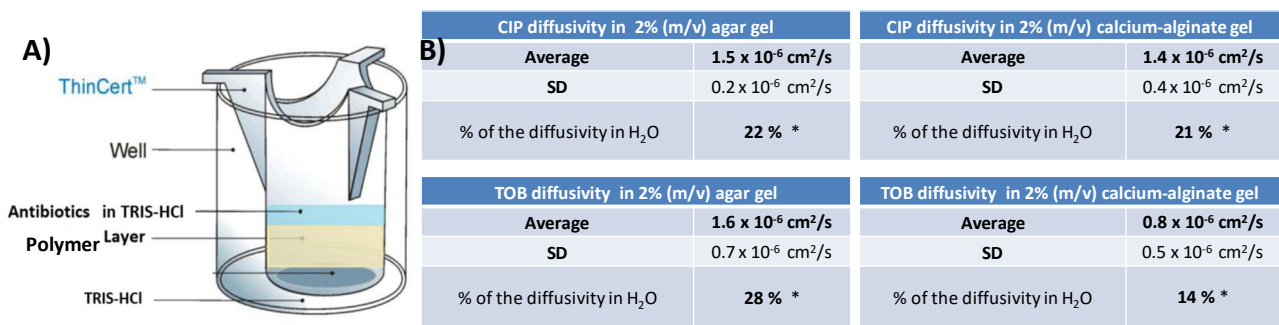


268
 269 **Figure 3: Luminescence kinetics obtained with *PAO1* freshly trapped in agar beads (solid lines) or for**
 270 **48 hours (dashed lines) before being dispersed in MHB containing different concentrations of TOB**
 271 **expressed in the number of times the MIC (Top of each graph). The blue horizontal curve (Control -**
 272 **) is the signal obtained in the absence of bacteria. For each well, luminescence intensity was**
 273 **normalized to the value measured at time zero. The gray band around the lines is the 95%**
 274 **confidence level interval of the mean values predicted from the GAM smoothing model (n=12-16).**
 275 **The mean values between different conditions are significantly different in the absence of**
 276 **overlapping of these gray-shaded areas.**

277 *PA*s freshly entrapped in calcium-alginate beads were less susceptible to TOB than those freshly
 278 entrapped in agar beads (Figure 2). However, in *in vivo* experiments, beads are instilled into the
 279 animals' lungs and are exposed to ATB only after 2-3 days when the bacterial burden is stable. During
 280 this period, *PAO1* can form biofilms in the beads that can influence the effect of ATB. To evaluate this,

281 luminescence kinetics using agar beads that did not appear to interfere with the TOB effect, were
 282 incubated for 48 hours in MHB prior to the addition of TOB. Luminescence kinetics measured from
 283 fresh or 48-hours-old agar beads were almost similar (Figure 3). PAs in 48-hours-old agar beads were
 284 slightly less susceptible to TOB than PAs in the fresh beads only for TOB concentration around the
 285 MIC. Additionally, PAs trapped into fresh or 48-hours-old agar beads were around 10 times more
 286 susceptible to TOB than PAs freshly trapped into calcium-alginate beads.

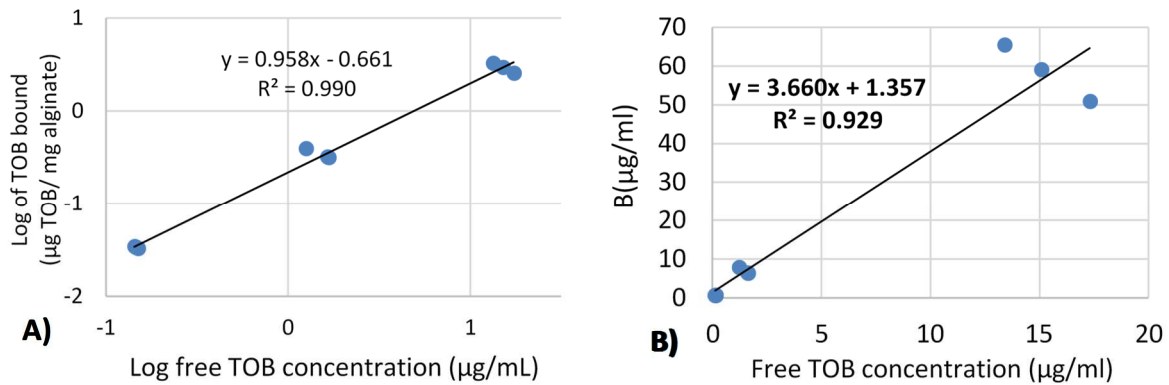
287 **Effective diffusivity of TOB and CIP in agar and calcium-alginate gels at 2% m/v.** To determine
 288 whether the decrease in the efficacy of TOB on PAs trapped in calcium-alginate beads compared to
 289 PAs trapped in agar beads could be due to a decrease in TOB diffusion, the effective diffusivity of the
 290 two ATBs were evaluated in both gels by measuring their transport rate through a layer of these gels
 291 (Figure 4).



292 **Figure 4: A) Scheme showing the test used to determine the ATBs effective diffusivities. B) CIP and**
 293 **TOB effective diffusivity values measured at 37°C in 2% (m/v) agar and 2% (m/v) calcium-alginate**
 294 **gels. * The diffusivity percentage of the two ATBs in the gels relative to their diffusivity in pure water**
 295 **was calculated using the diffusivity of the CIP in pure water ($6.9 \times 10^{-6} \text{ cm}^2/\text{s}$) and the diffusivity of**
 296 **TOB in pure water ($5.6 \times 10^{-6} \text{ cm}^2/\text{s}$) at 37°C obtained from Stewart [16].**

298 The CIP effective diffusivity values at 37°C were similar in both gels, with values of $1.5 \pm 0.2 \times 10^{-6} \text{ cm}^2/\text{s}$
 299 and $1.4 \pm 0.4 \times 10^{-6} \text{ cm}^2/\text{s}$ in 2% (m/v) agar and 2% (m/v) calcium-alginate gel, respectively (Figure 4).
 300 TOB effective diffusivity in agar gel ($1.6 \pm 0.7 \times 10^{-6} \text{ cm}^2/\text{s}$) was similar to that of CIP in this gel. In the
 301 calcium-alginate gel, the TOB effective diffusivity was reduced to $0.8 \pm 0.5 \times 10^{-6} \text{ cm}^2/\text{s}$. TOB interaction
 302 with the calcium-alginate gel was further investigated by measuring its binding at equilibrium with this
 303 gel. The concentration dependence of the TOB binding to 2% (m/v) calcium alginate gel was linear

304 within the concentration range tested (MIC at 100 times MIC - Figure 5A), which supposes the absence
 305 of saturation. Nichols *et al.* [14] also found a linear binding of TOB to sodium alginate in this range of
 306 TOB concentrations. The constant of proportionality between the amount of TOB bound to alginate
 307 and the free TOB concentration was around 3.7.

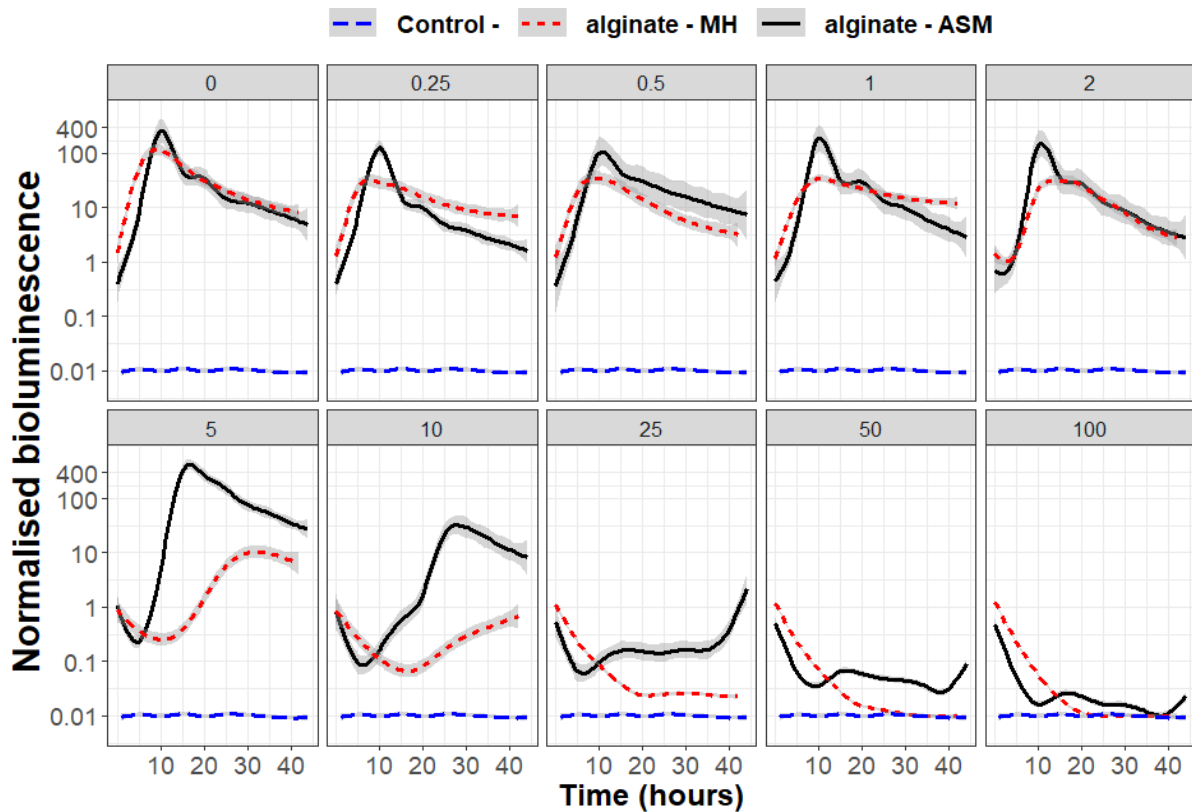


308 **Figure 5: Measurement of TOB binding to alginate. A) Log-log plot of the concentration dependence**
 309 **of TOB binding to calcium-alginate gel. B) Linear TOB adsorption isotherm described by $B = RC$,**
 310 **where B is the amount of TOB adsorbed in a unit volume ($\mu\text{g/ml}$), C is the free TOB concentration**
 311 **($\mu\text{g/ml}$), and R is the constant of proportionality.**

313 When adsorption reaches equilibrium instantaneously, solute effective diffusivity (De) in a gel can be
 314 related to its diffusivity in water by the following equation: $De = D(1 / (R + 1))$ [14]. Thus, using the
 315 diffusivity of TOB in the water at 37°C calculated from the Wilke-Chang correlation at $5.6 \times 10^{-6} \text{ cm}^2/\text{s}$
 316 [16], the effective diffusivity of TOB in the calcium-alginate gel was $1.2 \times 10^{-6} \text{ cm}^2/\text{s}$.

317 **Bioluminescence kinetics of PA entrapped calcium alginate beads dispersed in MHB or artificial**
 318 **sputum medium.** The effect of mucus components on the efficacy of TOB was accessed by measuring
 319 the luminescence kinetics of PA entrapped in calcium-alginate beads dispersed in artificial sputum
 320 medium (ASM) in the presence of different TOB concentrations (Figure 6). For TOB concentrations of
 321 up to 2 times the MIC, no difference was observed in the kinetics obtained with calcium-alginate beads
 322 dispersed in MHB or ASM. However, for TOB concentrations greater than 2 times the MIC and up to
 323 50 times the MIC, the ASM components further decreased the efficacy of the TOB compared to the
 324 results obtained with alginate-based beads dispersed in MHB. Higher luminescence values were

325 obtained in ASM and rebounds in the luminescence was observed after 40 hours for TOB
 326 concentrations up to 50 times the MIC.



327
 328 **Figure 6: Luminescence kinetics of *PAO1* obtained for different concentrations of TOB (expressed as**
 329 **a number of times the MIC against planktonic *PAO1*). *PAO1* were entrapped into calcium-alginate**
 330 **beads dispersed either in MH broth (dashed lines) or in artificial sputum medium (ASM) (solid lines).**
 331 **The blue horizontal curve (Control -) is the signal obtained in the absence of bacteria. For each well,**
 332 **luminescence intensity was normalized to the value measured at time zero. The gray band around**
 333 **the lines is the 95% confidence level interval of the mean values predicted from the GAM smoothing**
 334 **model (n=12-16). The mean values between different conditions are significantly different in the**
 335 **absence of overlapping of these gray-shaded areas.**

336 **4. Discussion**

337 *Pseudomonas aeruginosa (PA)* is responsible for pulmonary chronic infections in patients with chronic
 338 respiratory diseases such as cystic fibrosis (CF) and chronic obstructive pulmonary disease (COPD).
 339 These *PA* infections are usually associated with the presence of biofilms in the lungs that are
 340 impossible to eradicate [5, 17, 18]. This problem is worsening due to the occurrence of multidrug-
 341 resistance (MDR) *PA* worldwide [19]. In this context, new methodologies for treating these pulmonary

342 biofilms are being developed [20]. For example, new therapeutic approaches aim to improve the
343 penetration of ATBs into biofilm/mucus gels by ATB pegylation [12], or by loading them into
344 nanoparticles able to penetrate these gels [21, 22]. Some approaches aim at maintaining high ATB
345 concentration in the lung [23], optimizing ATBs dosage with PK-PD studies [4], or combining several
346 ATBs together or with anti-quorum sensing or biofilm dispersants [24]. To evaluate these strategies,
347 good *in vitro* and *in vivo* models simulating pulmonary biofilms conditions in human are central. The
348 two most common models used to create chronic pulmonary *PA* infections in rodents are pulmonary
349 instillation of *PA* confined in agar beads or calcium-alginate beads. To determine whether these two
350 beads models can be considered interchangeable, *PA*-loaded agar or calcium-alginate beads were
351 challenged with two clinically relevant ATBs, the TOB and the CIP, doing time-kill-like experiments. In
352 order to provide a high throughput-screening test for easy assessment of the ATB efficacy, a
353 bioluminescent *PAO1* was used.

354 **Use of bioluminescent bacteria seems an interesting tool to quickly evaluate the kinetics effect of**
355 **an antibiotic on bacteria grown either planktonically, as biofilms or immobilized within polymer**
356 **beads.** Time-kill curves are traditionally made by following the variation of concentration of bacteria
357 able to form a colony versus time. This method is time-consuming and allows only a limited number
358 of time points. For biofilms, it is even more complicated as you have to extract the bacteria from the
359 biofilm matrix [12, 24]. Monitoring the luminescence produced by transformed bacteria allows live
360 measurements and the acquisition of many points for precise kinetics. [25]. Still, bioluminescence is a
361 more complex parameter than a simple bacteria count as its value depends on the concentration of
362 living bacteria but also their metabolic state [26, 27]. Yet, bioluminescence permits the observation of
363 living bacteria that are metabolically active but unable to multiply to create a colony, such as bacteria
364 found in biofilms [26, 28]. One of the weaknesses of the use of bioluminescence could be the difficulty
365 to access the presence of persisters and ATB tolerant bacteria described in biofilms [29] that have low
366 or almost no metabolic activity and thus should produce much less light than the active bacteria.
367 Anyhow, persisters generally do not produce a visible colony in 20-24h and thus are normally not

368 detected by traditional time-kill experiments. Another limitation of the use of bioluminescence is the
369 needs of O₂ for the reaction that produce light. Studies have shown that O₂ diffusion can be limited in
370 alginate gels and biofilms [30-32]. Its penetration is generally limited to 50 to 90 μm down from the
371 surface of biofilms [30, 33]. Thus oxygen diffusion can be a restriction for using bioluminescence with
372 thick biofilms, as those formed on abiotic surfaces, or with large alginate beads [33], but for beads
373 having diameters lower than 100 μm, oxygen diffusion limitation should not be responsible for a
374 decrease in light production.

375 For adherent biofilms and planktonic cells, ATBs concentrations higher than the MIC induced a fast
376 decrease of the luminescence. This decrease was faster and more intense for planktonic *PAO1* than
377 for biofilms. Biofilm cells are less susceptible to antimicrobials than their planktonic counterparts [20,
378 29, 34]. Thus, the results obtained here are expected if the bioluminescence correlates with the
379 bacterial survival and metabolic state. The kinetics obtained with planktonic *PAO1*, adherent biofilms,
380 and with *PAs* entrapped in both types of beads displayed a concentration- and time-dependent change
381 in luminescence with both ATBs. Time-kill curves with similar behaviors were established with
382 planktonic *PAO1* treated with these two ATBs using the traditional bacterial counting method [35, 36].
383 Except for TOB in calcium-alginate beads, ATBs concentrations around the MIC induced an initial
384 decrease in luminescence that was followed by a rebound. In traditional time-kill experiments
385 performed with these ATBs at these concentrations, a “regrowth” of the bacterial population is often
386 observed [35, 36]. This observation is generally attributed either to the adaptation of bacteria to the
387 ATB (mutation) or to the selection of a subpopulation of bacteria that are already resistant but has a
388 slower growth rate than the majority of the bacteria in normal condition. This luminescence rebound
389 could be attributed to the growth of this kind of bacteria. For biofilms and for CIP concentrations
390 between 0.25 and 0.5 times the MIC, a higher normalized luminescence value was observed at the
391 plateau compared to the value obtained without ATB. This increase could be due to a stimulation of
392 the bacterial metabolism by CIP, as observed by other studies that showed that sub-MIC CIP
393 concentrations stimulate *PA* biofilm formation and virulence [37, 38].

394 **Agar and calcium-alginate beads are interchangeable for evaluating uncharged ATB such as the**
395 **fluoroquinolone CIP, but not for cationic aminoglycosides such as TOB.** Luminescence kinetics
396 obtained in the presence of a large range of CIP concentrations (0 to 100 times the MIC) were virtually
397 the same for *PAO1* trapped in calcium-alginate or agar beads. **The size distributions of the two types**
398 **of beads did not differ significantly, so their size should hardly influence the kinetic profiles.** Therefore,
399 both bead models seem interchangeable with CIP. For TOB however, a net difference was observed
400 between kinetics obtained from *PAs* entrapped in agar and calcium-alginate beads. In alginate beads,
401 *PAs* were up to 10 times less susceptible to TOB than in agar beads. **In these experiments, beads were**
402 **produced and immediately exposed to ATB. Initially, in these conditions, *PAs* entrapped are planktonic**
403 **bacteria.** Thus, at the beginning of the kinetics, the differences observed between the two types of
404 beads cannot be attributed to phenomena such as the presence of low metabolically active bacteria
405 found in biofilms. In addition, the effect of TOB on *PAs* entrapped freshly or for 2 days in agar beads
406 prior to addition of TOB was almost similar for all tested TOB concentrations. This suggests that *PAO1*
407 biofilm formed in agar beads had little effect on the TOB susceptibility compare to the effect of 2%
408 m/v calcium-alginate. Thus, when using non-mucoid bacteria such as *PAO1* that do not produce
409 alginate, the agar and calcium-alginate beads models are not interchangeable when testing cationic
410 ATB such as TOB.

411 The calcium-alginate beads model was developed based on the finding that many *PA* found in CF
412 patients are present as mucoid biofilms containing a large proportion of alginate in their EPS matrix.
413 Numerous studies evaluating the effect of ATBs on these biofilms have shown that their efficacies are
414 reduced compared to those obtained with free planktonic bacteria. Initially, it was thought that the
415 ATBs tolerance of bacteria in these biofilms was due to the limitation of ATBs transport in biofilms due
416 to the presence of the alginate-containing EPS matrix. [14, 39, 40]. So, the penetration of various ATBs
417 within biofilms of different *PAs*, or within calcium-alginate gels made from commercial seaweed
418 alginate or alginate from clinically relevant mucoid variants of *PA* was measured using various
419 methods [14, 39, 41-43]. With the exception of some positively charged ATBs, such as

420 aminoglycosides, which interact with negatively charged alginate [14, 39, 44-46] or calcium-alginate
421 [39], most ATBs, including CIP, readily penetrated biofilms and alginate gels at sufficiently high
422 velocities to exclude a limiting phenomenon that would contribute to antimicrobial tolerance [14, 39,
423 44]. Even though TOB penetration in alginate-based biofilms is delayed [42], some studies considered
424 to have a minor effect on the ATB tolerance [47]. In our study, the effective diffusivity of CIP at 37°C
425 calculated from transport experiments through both gels was around $1.5 \times 10^{-6} \text{ cm}^2/\text{s}$, which is 5 times
426 lower than its value in water [16]. Even with this reduction, luminescence kinetics obtained in the
427 presence of CIP with both types of beads were highly similar to those obtained with planktonic
428 bacteria. TOB effective diffusivity in agar ($1.6 \pm 0.7 \times 10^{-6} \text{ cm}^2/\text{s}$) was close to that of the CIP in this gel
429 and was reduced by 3.5 fold in relation to its diffusivity in water. This effective diffusivity was 2 times
430 lower than the value found by Gordon *et al.* [39] in a similar 2% m/v agar gels ($3.0 \times 10^{-6} \text{ cm}^2/\text{s}$). TOB
431 effective diffusivity in 2% (m/v) calcium-alginate gel ($0.8 \pm 0.5 \times 10^{-6} \text{ cm}^2/\text{s}$) was 2 times lower than in
432 2% (m/v) agar gel and 7 times lower than in water [16]. This value was in the same range than the
433 value found by Gordon *et al.* [39] in 2% (m/v) alginate containing calcium lactate as a gelling agent
434 ($0.65 \pm \times 10^{-6} \text{ cm}^2/\text{s}$). TOB diffusivity in the calcium-alginate gel was also assessed from its binding at
435 equilibrium to this gel as described by Nichols *et al.* [14]. It was evaluated at $1.2 \times 10^{-6} \text{ cm}^2/\text{s}$, which is
436 in the same range of values as calculated from the transport experiment across a calcium-alginate gel
437 layer. According to Stewart, P. S. [47] and Nichols *et al.* [14], the time required for a molecule to
438 achieve 90% of the dispersing medium concentration at the center of a spherical polymer bead is
439 estimated by $t_{90} = 0.37 \times R^2/De$, where R is the radius of the bead and De is the effective diffusivity
440 of the molecule in the polymer. Therefore, with a diffusivity of $0.8 \pm 0.5 \times 10^{-6} \text{ cm}^2/\text{s}$ and beads having
441 a maximal diameter of 100 μm , 12 seconds should be needed for TOB to obtain 90% of the dispersing
442 medium concentration at the center of beads. Thus, only a decrease in the diffusivity of TOB in alginate
443 by a factor of 1000 to 10,000 could explain by itself the difference in efficacy against *PAO1* entrapped
444 in calcium-alginate compared with those trapped in agar.

445 The reduction of TOB diffusivity seems not a major mechanism of TOB resistance of *PA* in calcium-
446 alginate beads. However, several studies proposed that the delay in TOB penetration give to the
447 bacteria the time to adapt to the ATB and adopt a more antimicrobial-tolerant state before killing
448 concentrations of the ATB can be achieved [48]. In agreement with this suggestion, hydrolysis of
449 alginate by alginate lyase enhanced the activity of TOB in biofilms by dissolving the biofilm matrix [49].
450 Also, *PA* exposures to sub-lethal concentrations of TOB results in phenotypic alterations such as
451 increased EPS productions or activation of ATB efflux pump [50].

452 **Alginate beads dispersed in artificial sputum media could be a good model to simulate pulmonary**
453 **biofilms.** In cystic fibrosis (CF) patients, the conductive zone serves as a bacterial reservoir where the
454 bacteria are organized in mucoid biofilms within the mucus, protected against ATBs and host defenses
455 [5]. These two gels that are biofilm and mucus are formed of negatively charged polymers that could
456 behave as barrier able to reversibly bind cationic ATBs and slow down their penetration [12, 51]. This
457 reduction in ATBs penetration rate could give the bacteria enough time to adapt to the ATBs [40, 48].
458 *In vivo PA* biofilm patches found in the pulmonary mucus of chronically infected CF patients have sizes
459 ranged from 5 to 200 μm in diameter [5, 18, 52]. With a high frequency, *PA*s found in these infections
460 are able to create mucoid biofilms having a high concentration in alginate [34]. Thus, alginate beads
461 having the size of the biofilm clusters found in the CF patients lungs dispersed in mucus or mucus-
462 simulating medium could be a good model for evaluating anti-biofilm strategies. In the present study,
463 we have shown that the dispersion of the alginate beads in ASM further reduced the efficacy of TOB
464 compared to the same beads dispersed in MHB. This result is in agreement with Müller *et al.* [45]
465 study showing a significant reduction of TOB efficacy against *PA* biofilms grown on 96-well plates in
466 the presence of mucus compared with those grown in the absence of mucus. Also, several studies
467 have shown that the presence of mucus altered the *PA* biofilms behaviors [53] and promote the
468 expression of several genes responsible for ATB resistance [54, 55].

469 In human, most planktonic bacteria are killed by the ATB and the residual bacteria are eradicated by
470 the immune system. For biofilms, however, due to the presence of the EPS matrix, immune cells

471 cannot reach the bacteria and the residual cells that are not killed by the ATB might be able to restore
472 the biofilm. Also, bacteria in biofilms are less susceptible to ATBs than their planktonic counterparts.
473 Therefore, ATB concentrations required to eradicate bacterial infections with biofilms are higher than
474 the clinical targets usually used to treat infections caused by planktonic cells. These concentrations
475 are difficultly achievable via systemic administration and pulmonary biofilms eradication seems only
476 possible by ATB inhalation due to the possibility to achieve high ATB concentrations in biofilms while
477 avoiding side effects and toxicity. The mucus barrier is often neglected in *in vitro* tests employed to
478 evaluate the efficacy of inhaled ATBs. This model could be highly relevant in testing the efficacy of
479 inhaled ATB, whose development to treat pulmonary lung infections is increasing [21, 56].

480 In CF patients, activated polymorphonuclear leukocytes (PMNs) are accumulating around the bacterial
481 aggregates [5]. PMNs impact on *PAs* behavior and release a large amount of extracellular DNA that
482 could affect cationic ATB efficacy [57, 58]. Thus, a model using small beads of calcium-alginate
483 dispersed in medium simulating mucus could be supplemented with immune cell lines that could
484 aggregate around the beads, which would make it possible to study the effect of the three barriers
485 (biofilm, mucus, and agglomerated immune cells) that an ATB must pass to reach the bacteria.

486 **5. Conclusion**

487 These results show that the agar and alginate beads models can be interchangeable only for
488 uncharged ATB, such as CIP, but not for all ATB. *In vitro* experiments performed in this study could be
489 a quick way to evaluate the influence of each model on a given ATB before performing animal
490 experiments.

491 **6. References**

- 492 [1] H. Cash, D. Woods, B. McCullough, W. Johanson Jr, J. Bass, A rat model of chronic respiratory
493 infection with *Pseudomonas aeruginosa*, *American Review of Respiratory Disease*, 119 (1979) 453-
494 459.
- 495 [2] E. Growcott, A. Coulthard, R. Amison, E. Hardaker, V. Saxena, L. Malt, P. Jones, A. Grevot, C. Poll,
496 C. Osborne, Characterisation of a refined rat model of respiratory infection with *Pseudomonas*
497 *aeruginosa* and the effect of ciprofloxacin, *Journal of Cystic Fibrosis*, 10 (2011) 166-174.
- 498 [3] J. Lam, R. Chan, K. Lam, J. Costerton, Production of mucoid microcolonies by *Pseudomonas*
499 *aeruginosa* within infected lungs in cystic fibrosis, *Infection and immunity*, 28 (1980) 546-556.
- 500 [4] B.G.S. Torres, V.E. Helfer, P.M. Bernardes, A.J. Macedo, E.I. Nielsen, L.E. Friberg, T. Dalla Costa,
501 Population pharmacokinetic modeling as a tool to characterize the decrease in ciprofloxacin free
502 interstitial levels caused by *pseudomonas aeruginosa* biofilm lung infection in wistar rats,
503 *Antimicrobial agents and chemotherapy*, 61 (2017) e02553-02516.
- 504 [5] T. Bjarnsholt, P.Ø. Jensen, M.J. Fiandaca, J. Pedersen, C.R. Hansen, C.B. Andersen, T. Pressler, M.
505 Givskov, N. Høiby, *Pseudomonas aeruginosa* biofilms in the respiratory tract of cystic fibrosis patients,
506 *Pediatric pulmonology*, 44 (2009) 547-558.
- 507 [6] H. Bayes, N. Ritchie, S. Irvine, T. Evans, A murine model of early *Pseudomonas aeruginosa* lung
508 disease with transition to chronic infection, *Scientific reports*, 6 (2016) 1-10.
- 509 [7] S. Gandi, I. Cranston, G. Mclachlan, S. Wright, J. Baily, S. Stimpson, S. Madden, M. Whitmarsh, A.
510 Young, M. Mcelroy, Effects of direct lung dosing of Tobramycin in a rat chronic infection model using
511 *Pseudomonas aeruginosa* RP73, *European Respiratory Journal*, 52 (2018) 2656.
- 512 [8] W. Hengzhuang, K. Green, T. Pressler, M. Skov, T.L. Katzenstein, X. Wu, N. Høiby, Optimization of
513 colistin dosing regimen for cystic fibrosis patients with chronic *Pseudomonas aeruginosa* biofilm lung
514 infections, *Pediatric pulmonology*, 54 (2019) 575-580.
- 515 [9] D.-j. Kim, S.-g. Chung, S.-h. Lee, J.-w. Choi, Relation of microbial biomass to counting units for
516 *Pseudomonas aeruginosa*, *African Journal of Microbiology Research*, 6 (2012) 4620-4622.
- 517 [10] T. Jouenne, O. Tresse, G.-A. Junter, Agar-entrapped bacteria as an in vitro model of biofilms and
518 their susceptibility to antibiotics, *FEMS microbiology letters*, 119 (1994) 237-242.
- 519 [11] A. Braun, K. Sewald, L. Müller, S. Wronski, X. Murgia, C.-M. Lehr, C. Börger, L. Siebenbürger, M.
520 Hittinger, K. Schwarzkopf, S. Häussler, Human airway mucus alters susceptibility of *Pseudomonas*
521 *aeruginosa* biofilms to tobramycin, but not colistin, *Journal of Antimicrobial Chemotherapy*, 73 (2018)
522 2762-2769.
- 523 [12] T.F. Bahamondez-Canas, H. Zhang, F. Tewes, J. Leal, H.D. Smyth, PEGylation of tobramycin
524 improves mucus penetration and antimicrobial activity against *Pseudomonas aeruginosa* biofilms in
525 vitro, *Molecular pharmaceutics*, 15 (2018) 1643-1652.
- 526 [13] S.D. Dinesh, Artificial sputum medium, *Protoc. exch*, (2010).
- 527 [14] W. Nichols, S. Dorrington, M. Slack, H. Walmsley, Inhibition of tobramycin diffusion by binding to
528 alginate, *Antimicrobial agents and chemotherapy*, 32 (1988) 518-523.
- 529 [15] S. Marchand, N. Grégoire, J. Brillault, I. Lamarche, P. Gobin, W. Couet, Biopharmaceutical
530 Characterization of Nebulized Antimicrobial Agents in Rats: 3. Tobramycin, *Antimicrobial Agents and*
531 *Chemotherapy*, 59 (2015) 6646-6647.
- 532 [16] P.S. Stewart, Theoretical aspects of antibiotic diffusion into microbial biofilms, *Antimicrobial*
533 *agents and chemotherapy*, 40 (1996) 2517-2522.

- 534 [17] N. Høiby, O. Ciofu, T. Bjarnsholt, *Pseudomonas aeruginosa* biofilms in cystic fibrosis, *Future*
535 *microbiology*, 5 (2010) 1663-1674.
- 536 [18] T. Bjarnsholt, The role of bacterial biofilms in chronic infections, *Apmis*, 121 (2013) 1-58.
- 537 [19] K.M. Langan, T. Kotsimbos, A.Y. Peleg, Managing *Pseudomonas aeruginosa* respiratory infections
538 in cystic fibrosis, *Current opinion in infectious diseases*, 28 (2015) 547-556.
- 539 [20] H. Wu, C. Moser, H.-Z. Wang, N. Høiby, Z.-J. Song, Strategies for combating bacterial biofilm
540 infections, *International Journal Of Oral Science*, 7 (2014) 1.
- 541 [21] N. Günday Türeli, A. Torge, J. Juntke, B.C. Schwarz, N. Schneider-Daum, A.E. Türeli, C.-M. Lehr, M.
542 Schneider, Ciprofloxacin-loaded PLGA nanoparticles against cystic fibrosis *P. aeruginosa* lung
543 infections, *European Journal of Pharmaceutics and Biopharmaceutics*, 117 (2017) 363-371.
- 544 [22] J. Ernst, M. Klinger-Strobel, K. Arnold, J. Thamm, A. Hartung, M.W. Pletz, O. Makarewicz, D.
545 Fischer, Polyester-based particles to overcome the obstacles of mucus and biofilms in the lung for
546 tobramycin application under static and dynamic fluidic conditions, *European Journal of*
547 *Pharmaceutics and Biopharmaceutics*, 131 (2018) 120-129.
- 548 [23] B. Lamy, F. Tewes, D.R. Serrano, I. Lamarche, P. Gobin, W. Couet, A.M. Healy, S. Marchand, New
549 aerosol formulation to control ciprofloxacin pulmonary concentration, *Journal of Controlled Release*,
550 271 (2018) 118-126.
- 551 [24] H. Bandara, M. Herpin, D. Kolacny Jr, A. Harb, D. Romanovicz, H. Smyth, Incorporation of farnesol
552 significantly increases the efficacy of liposomal ciprofloxacin against *Pseudomonas aeruginosa*
553 biofilms in vitro, *Molecular pharmaceutics*, 13 (2016) 2760-2770.
- 554 [25] R. Thorn, S. Nelson, J. Greenman, Use of a bioluminescent *Pseudomonas aeruginosa* strain within
555 an in vitro microbiological system, as a model of wound infection, to assess the antimicrobial efficacy
556 of wound dressings by monitoring light production, *Antimicrobial agents and chemotherapy*, 51 (2007)
557 3217-3224.
- 558 [26] C.N.H. Marques, S.M. Nelson, Pharmacodynamics of ciprofloxacin against *Pseudomonas*
559 *aeruginosa* planktonic and biofilm-derived cells, *Letters in Applied Microbiology*, 68 (2019) 350-359.
- 560 [27] C.N. Marques, V.C. Salisbury, J. Greenman, K.E. Bowker, S.M. Nelson, Discrepancy between viable
561 counts and light output as viability measurements, following ciprofloxacin challenge of self-
562 bioluminescent *Pseudomonas aeruginosa* biofilms, *Journal of Antimicrobial Chemotherapy*, 56 (2005)
563 665-671.
- 564 [28] C. Fux, J.W. Costerton, P.S. Stewart, P. Stoodley, Survival strategies of infectious biofilms, *Trends*
565 *in microbiology*, 13 (2005) 34-40.
- 566 [29] P.S. Stewart, Mechanisms of antibiotic resistance in bacterial biofilms, *International Journal of*
567 *Medical Microbiology*, 292 (2002) 107-113.
- 568 [30] M. Sønderholm, K.N. Kragh, K. Koren, T.H. Jakobsen, S.E. Darch, M. Alhede, P.Ø. Jensen, M.
569 Whiteley, M. Kühn, T. Bjarnsholt, *Pseudomonas aeruginosa* aggregate formation in an alginate bead
570 model system exhibits in vivo-like characteristics, *Appl. Environ. Microbiol.*, 83 (2017) e00113-00117.
- 571 [31] D.J. Hassett, Anaerobic production of alginate by *Pseudomonas aeruginosa*: alginate restricts
572 diffusion of oxygen, *Journal of Bacteriology*, 178 (1996) 7322-7325.
- 573 [32] B. Pabst, B. Pitts, E. Lauchnor, P.S. Stewart, Gel-entrapped *Staphylococcus aureus* bacteria as
574 models of biofilm infection exhibit growth in dense aggregates, oxygen limitation, antibiotic tolerance,
575 and heterogeneous gene expression, *Antimicrobial agents and chemotherapy*, 60 (2016) 6294-6301.
- 576 [33] M. Sønderholm, K. Koren, D. Wangpraseurt, P.Ø. Jensen, M. Kolpen, K.N. Kragh, T. Bjarnsholt, M.
577 Kühn, Tools for studying growth patterns and chemical dynamics of aggregated *Pseudomonas*

578 aeruginosa exposed to different electron acceptors in an alginate bead model, npj Biofilms and
579 Microbiomes, 4 (2018) 3.

580 [34] N. Høiby, T. Bjarnsholt, M. Givskov, S. Molin, O. Ciofu, Antibiotic resistance of bacterial biofilms,
581 International Journal of Antimicrobial Agents, 35 (2010) 322-332.

582 [35] J.B. Bulitta, N.S. Ly, C.B. Landersdorfer, N.A. Wanigaratne, T. Velkov, R. Yadav, A. Oliver, L. Martin,
583 B.S. Shin, A. Forrest, B.T. Tsuji, Two Mechanisms of Killing of *Pseudomonas aeruginosa* by Tobramycin
584 Assessed at Multiple Inocula via Mechanism-Based Modeling, Antimicrobial Agents and
585 Chemotherapy, 59 (2015) 2315-2327.

586 [36] N. Grégoire, S. Raherison, C. Grignon, E. Comets, M. Marliat, M.-C. Ploy, W. Couet,
587 Semimechanistic pharmacokinetic-pharmacodynamic model with adaptation development for time-
588 kill experiments of ciprofloxacin against *Pseudomonas aeruginosa*, Antimicrobial agents and
589 chemotherapy, 54 (2010) 2379-2384.

590 [37] J.F. Linares, I. Gustafsson, F. Baquero, J. Martinez, Antibiotics as intermicrobial signaling agents
591 instead of weapons, Proceedings of the National Academy of Sciences, 103 (2006) 19484-19489.

592 [38] F. Tewes, T.F. Bahamondez-Canas, H.D.C. Smyth, Efficacy of Ciprofloxacin and its Copper Complex
593 against *Pseudomonas aeruginosa* Biofilms, AAPS PharmSciTech, 20 (2019) 205-214.

594 [39] C.A. Gordon, N.A. Hodges, C. Marriott, Antibiotic interaction and diffusion through alginate and
595 exopolysaccharide of cystic fibrosis-derived *Pseudomonas aeruginosa*, Journal of Antimicrobial
596 Chemotherapy, 22 (1988) 667-674.

597 [40] B.S. Tseng, W. Zhang, J.J. Harrison, T.P. Quach, J.L. Song, J. Penterman, P.K. Singh, D.L. Chopp, A.I.
598 Packman, M.R. Parsek, The extracellular matrix protects *Pseudomonas aeruginosa* biofilms by limiting
599 the penetration of tobramycin, Environmental Microbiology, 15 (2013) 2865-2878.

600 [41] M. Shigeta, G. Tanaka, H. Komatsuzawa, M. Sugai, H. Suginaka, T. Usui, Permeation of
601 antimicrobial agents through *Pseudomonas aeruginosa* biofilms: a simple method, Chemotherapy, 43
602 (1997) 340-345.

603 [42] M.C. Walters, F. Roe, A. Bugnicourt, M.J. Franklin, P.S. Stewart, Contributions of antibiotic
604 penetration, oxygen limitation, and low metabolic activity to tolerance of *Pseudomonas aeruginosa*
605 biofilms to ciprofloxacin and tobramycin, Antimicrobial agents and chemotherapy, 47 (2003) 317-323.

606 [43] L. Coquet, G. Junter, T. Jouenne, Resistance of artificial biofilms of *Pseudomonas aeruginosa* to
607 imipenem and tobramycin, The Journal of antimicrobial chemotherapy, 42 (1998) 755-760.

608 [44] R.A. Hatch, N.L. Schiller, Alginate Lyase Promotes Diffusion of Aminoglycosides through the
609 Extracellular Polysaccharide of *MucoidPseudomonas aeruginosa*, Antimicrobial agents and
610 chemotherapy, 42 (1998) 974-977.

611 [45] L. Müller, X. Murgia, L. Siebenbürger, C. Börger, K. Schwarzkopf, K. Sewald, S. Häussler, A. Braun,
612 C.-M. Lehr, M. Hittinger, Human airway mucus alters susceptibility of *Pseudomonas aeruginosa*
613 biofilms to tobramycin, but not colistin, Journal of Antimicrobial Chemotherapy, 73 (2018) 2762-2769.

614 [46] M. Heriot, B. Nottelet, X. Garric, M. D'Este, G.R. Richards, F.T. Moriarty, D. Eglin, O. Guillaume,
615 Interaction of gentamicin sulfate with alginate and consequences on the physico-chemical properties
616 of alginate-containing biofilms, International Journal of Biological Macromolecules, 121 (2019) 390-
617 397.

618 [47] P.S. Stewart, Diffusion in biofilms, Journal of bacteriology, 185 (2003) 1485-1491.

619 [48] B. Cao, L. Christophersen, M. Kolpen, P.Ø. Jensen, K. Sneppen, N. Høiby, C. Moser, T. Sams,
620 Diffusion retardation by binding of tobramycin in an alginate biofilm model, PloS one, 11 (2016)
621 e0153616.

- 622 [49] M. Alipour, Z.E. Suntres, A. Omri, Importance of DNase and alginate lyase for enhancing free and
623 liposome encapsulated aminoglycoside activity against *Pseudomonas aeruginosa*, *Journal of*
624 *Antimicrobial Chemotherapy*, 64 (2009) 317-325.
- 625 [50] L.R. Hoffman, D.A. D'Argenio, M.J. MacCoss, Z. Zhang, R.A. Jones, S.I. Miller, Aminoglycoside
626 antibiotics induce bacterial biofilm formation, *Nature*, 436 (2005) 1171-1175.
- 627 [51] J. Witten, T. Samad, K. Ribbeck, Molecular characterization of mucus binding, *Biomacromolecules*,
628 20 (2019) 1505-1513.
- 629 [52] T. Bjarnsholt, M. Alhede, M. Alhede, S.R. Eickhardt-Sørensen, C. Moser, M. Kühl, P.Ø. Jensen, N.
630 Høiby, The in vivo biofilm, *Trends in microbiology*, 21 (2013) 466-474.
- 631 [53] C.L. Haley, J.A. Colmer-Hamood, A.N. Hamood, Characterization of biofilm-like structures formed
632 by *Pseudomonas aeruginosa* in a synthetic mucus medium, *BMC microbiology*, 12 (2012) 181.
- 633 [54] R.M. Landry, D. An, J.T. Hupp, P.K. Singh, M.R. Parsek, Mucin–*Pseudomonas aeruginosa*
634 interactions promote biofilm formation and antibiotic resistance, *Molecular microbiology*, 59 (2006)
635 142-151.
- 636 [55] S. Lory, S. Jin, J.M. Boyd, J.L. Rakeem, P. Bergman, Differential gene expression by *Pseudomonas*
637 *aeruginosa* during interaction with respiratory mucus, *American journal of respiratory and critical care*
638 *medicine*, 154 (1996) S183.
- 639 [56] P.P.H. Le Brun, A.H. de Boer, G.P.M. Mannes, D.M.I. de Fraiture, R.W. Brimicombe, D.J. Touw, A.A.
640 Vinks, H.W. Frijlink, H.G.M. Heijerman, Dry powder inhalation of antibiotics in cystic fibrosis therapy:
641 part 2: Inhalation of a novel colistin dry powder formulation: a feasibility study in healthy volunteers
642 and patients, *European Journal of Pharmaceutics and Biopharmaceutics*, 54 (2002) 25-32.
- 643 [57] W.-C. Chiang, M. Nilsson, P.Ø. Jensen, N. Høiby, T.E. Nielsen, M. Givskov, T. Tolker-Nielsen,
644 Extracellular DNA shields against aminoglycosides in *Pseudomonas aeruginosa* biofilms, *Antimicrobial*
645 *agents and chemotherapy*, 57 (2013) 2352-2361.
- 646 [58] H. Mulcahy, L. Charron-Mazenod, S. Lewenza, Extracellular DNA chelates cations and induces
647 antibiotic resistance in *Pseudomonas aeruginosa* biofilms, *PLoS Pathog*, 4 (2008) e1000213.

